ChemComm

COMMUNICATION

View Article Online
View Journal



Cite this: DOI: 10.1039/d5cc05870h

Received 15th October 2025,
Accepted 4th December 2025

DOI: 10.1039/d5cc05870h

rsc.li/chemcomm

# Annulated oxazolium salts as anion–$\pi^+$ interaction-enabled solid-state room-temperature phosphorescent materials

Shivankar Jagota,† Samim Sohel Rana,† Chhotan Barman and Joyanta Choudhury *

**Efficient counter-anion exchange represents a powerful and straightforward approach for modulating the photophysical properties of ionic luminescent materials without structural modification. Herein, we report how fluorescent annulated oxazolium salts switched to room-temperature phosphorescent materials upon counter-anion exchange of hexafluorophosphate ($PF_6^-$) with iodide ($I^-$).**

The domain of molecular interactions is an intriguing sphere where minute forces dictate the behaviour and characteristics of materials at a fundamental level. The "anion–$\pi^+$ interaction" has become a phenomenon of significant importance in chemistry, biology, and materials science. This interesting interaction involves attractive forces between a negatively charged ion (anion) and a positively charged region within a π electron cloud, commonly seen in aromatic systems.[1] In contrast to cation–π interactions, anion–$\pi^+$ interactions were unrecognised for many years because of their inherently repulsive characteristics, due to the "anion–π-electron cloud" interaction component. However, these interactions are notable when the aromatic systems are electron-deficient, specifically when positively charged, or electron-withdrawing groups are attached to the π-systems.[2,3] Anion–$\pi^+$ interactions can precisely modulate the emission of luminogens due to the close proximity of anions to aromatic π-systems, particularly *via* influencing intermolecular stacking and acting as barriers that inhibit π–π stacking in aggregation-induced emission (AIE) systems.[4] Interestingly, the introduction of variable anions to the positively charged aromatic systems results in the emergence of unique characteristics through variable anion–$\pi^+$ interactions. For instance, room temperature phosphorescence (RTP) is one such property that is induced by heavier anions like bromide ($Br^-$) and iodide ($I^-$). Organic RTP materials have received a lot of research interest due to their potential in a wide range of optoelectronic applications. The presence of these heavy counter-anions exerts an external heavy atom effect (EHE), which enhances spin–orbit coupling (SOC) and facilitates efficient intersystem crossing (ISC), thereby enabling room temperature phosphorescence (Fig. 1a). Inspired by this concept, a series of quinolinium derivatives,[5] 1,2,3,4-tetraphenyloxazolium salts,[6] and pyridinium salts,[7] with different heavy halide counter-anions ($Br^-$ and $I^-$), were developed as solid-state RTP materials (Fig. 1b). The strategy has also been extended to electron-deficient dicationic pyromellitic diimide derivatives,[8] and

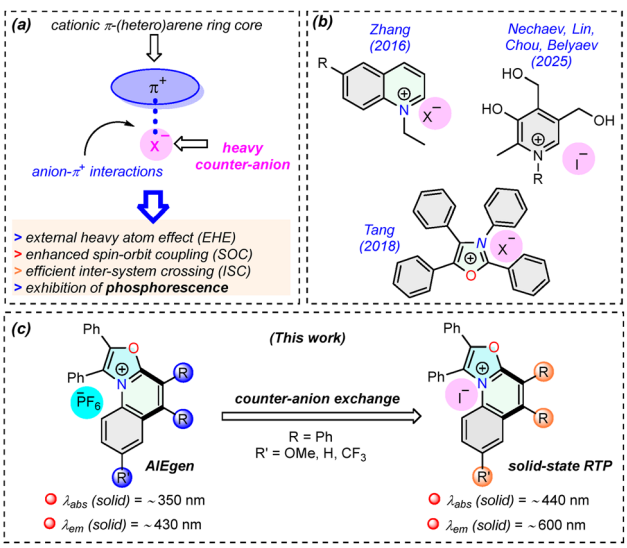


Fig. 1 (a) Heavy counter-anion–$\pi^+$ interaction-enabled process of phosphorescence emission. (b) Previously reported heavy counter-anion–$\pi^+$ interaction-enabled room-temperature phosphorescent compounds. (c) This work: counter-anion exchange-based modulation of absorption–emission properties of ring-fused annulated oxazolium salts.

*Organometallics & Smart Materials Laboratory, Department of Chemistry, Indian Institute of Science Education and Research (IISER) Bhopal, Bhopal 462 066, India. E-mail: joyanta@iiserb.ac.in*

† These authors contributed equally.

conjugated arene spacer-containing diphosphonium salts,[9] to design new solid-state RTP-based luminescent materials.

While developing novel annulated azolium salts with diverse functionality and applications,[10–17] recently, our group designed a new class of anion–$\pi^+$ AIEgens based on ring-fused annulated oxazoliums having hexafluorophosphate ($PF_6^-$) as a counter-anion.[18] These ring-fused oxazoliums are highly emissive and exhibit AIE properties in the THF/hexane mixture. All the cationic AIEgens exhibited strong fluorescence in the solid state, and functional groups on the tricyclic backbone had a significant impact on tuning the emission property of these fluorophores in the solid state (Fig. 1c).[18] In the present work, we envisaged to alter the emission property of these ring-fused annulated oxazoliums by exchanging the counter-anion $PF_6^-$ with the heavier counterpart $I^-$, by harnessing the EHE through counter-anion–$\pi^+$ interactions, and thus to switch these solid-state fluorescent compounds into solid-state RTP materials (Fig. 1c).

The ring-fused annulated oxazolium AIEgens with the $PF_6^-$ counter-anion, **1-PF$_6$**, **2-PF$_6$**, and **3-PF$_6$**, synthesized previously by employing our 'oxazolium-APEX' approach (APEX = annulative π-expansion),[18] were subjected to counter-anion exchange from hexafluorophosphate to iodide. Briefly, the oxazolium salts were stirred with 1.2 equivalents of tetrabutylammonium iodide (TBAI) in methanol for 2 hours at room temperature. During this period, the colour of the solid samples changed from off-white to yellowish. Furthermore, washing the resulting precipitate with diethyl ether and *n*-hexane furnished pure oxazolium salts with iodide as the counter-anion, **1-I**, **2-I**, and **3-I**. The iodide salts were fully characterised by $^1$H and $^{13}$C NMR spectroscopy, ESI-HRMS, and SC-XRD analysis (see the SI).

The solid-state emission of the iodide compounds markedly differed from that of the hexafluorophosphate compounds; under UV-Vis light irradiation, they emitted yellow to reddish colours, contingent upon the substituents linked to the annulated oxazolium backbone (Fig. 2a–c). Interestingly, the counter-anion exchange of the iodide compounds reversibly back to the hexafluorophosphate systems was also found to be very facile in an acetonitrile–water mixture at ambient temperature. Of note, this reversible $PF_6^-$ ↔ $I^-$ counter-anion exchange phenomenon might also be advantageous for chemosensory AIE in anion detection.[19]

Next, we examined the photophysical properties of **1-I**, **2-I**, and **3-I** in detail (Table 1). UV-Vis spectroscopy was performed on these compounds in various solvents ranging from non-polar to polar, and no changes in the absorption maxima ($\lambda_{max}$) were observed when changing the counter-anion from hexafluorophosphate to iodide; however, in the solid state, $\lambda_{max}$ shifted from the range of 347–357 nm to the range of 438–448 nm (Fig. S13, SI). In the solid state, the emission maxima ($\lambda_{em}$) of the iodide compounds, when excited at around 440 nm, appeared near 600 nm (Fig. 3a). The reversibility of counter-anion exchange was confirmed by the consistent solid-state emissions at 432 nm and 586 nm for the representative **2-PF$_6$** and **2-I**, respectively, over six cycles (Fig. 3b). The lifetime of the iodide compounds in dichloromethane solution was less than 1 ns;

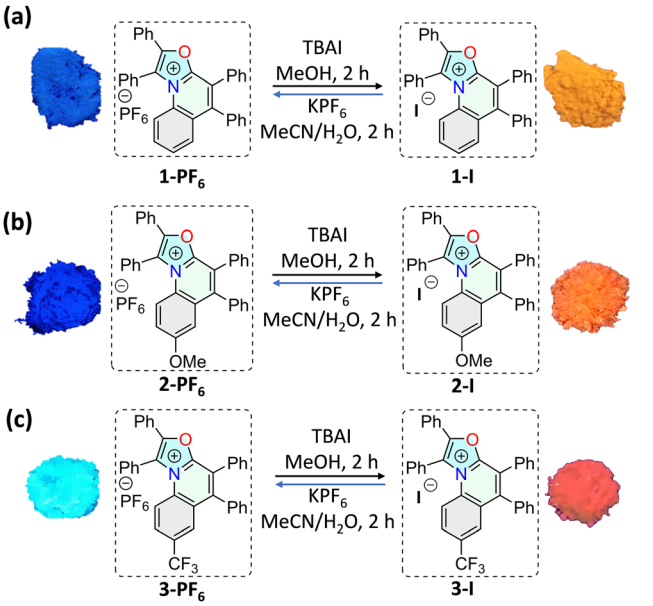


Fig. 2 (a)–(c) Reversible counter-anion exchange of **1-PF$_6$**, **2-PF$_6$** **3-PF$_6$**/**1-I**, **2-I**, and **3-I**. Photographs on the left and right display the solid-state emission colours of the compounds.

Table 1 Photophysical properties of **1-I**, **2-I** and **3-I**

| | $\lambda_{abs}$ (nm) | | $\lambda_{em}$ (nm) | | $\tau_{av}$ [b] (ns) | |
|---|---|---|---|---|---|---|
| # | Solution[a] | Solid | Solution[a] | Solid | Solution[a] | Solid |
| **1-I** | 350 | 442 | 430 | 593 | 0.16 | 28 650 |
| **2-I** | 347 | 438 | 432 | 586 | 0.47 | 25 290 |
| **3-I** | 357 | 448 | 437 | 597 | 0.75 | 31 120 |

[a] In dichloromethane. [b] Average lifetime.

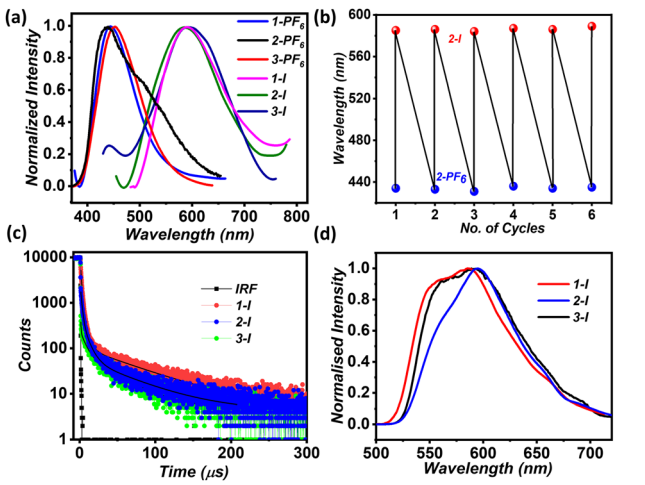


Fig. 3 (a) Solid-state photoluminescence (PL) spectra of **1-PF$_6$**, **2-PF$_6$**, **3-PF$_6$**/**1-I**, **2-I**, and **3-I** pairs. (b) Reversible counter-anion exchange of **2-PF$_6$**/**2-I** pairs up to 6 cycles. (c) Time-resolved PL decay of the iodide compounds in the solid state at room temperature. (d) The delayed PL spectra of the iodide compounds at 77 K.

however, it increased to more than 25 μs when recorded in the solid state (Fig. 3c and Table 1). This indicated the phosphorescence-type emission. Consequently, we assessed the phosphorescence of the compounds. These compounds displayed weak phosphorescence spectra in dichloromethane solution at room temperature; however, when the spectra were recorded at 77 K, all iodide compounds exhibited intense phosphorescence (Fig. 3d). In the solid state, all these compounds showed intense phosphorescence under air at room temperature (Fig. S26, SI). The notable shift in the absorption and emission maxima, caused by counter-anion exchange, is significant in this class of compounds. The solution-state emission of the iodide compounds appeared at ~430 nm, while in the solid state, the emission maximum shifted to ~600 nm. In contrast, the emission maximum of the hexafluorophosphate molecules remained steady at ~440 nm, due to their blue or cyan emission in solution as well as in the solid state.

Furthermore, the density functional theory (DFT) calculations of the iodide compounds demonstrated that the highest occupied molecular orbital (HOMO) was localised on the iodide and the lowest unoccupied molecular orbital (LUMO) was localised on the cationic π-system. The HOMO was positioned over the iodide anion due to the higher-lying non-bonding frontier orbitals of iodine. Consequently, they dominate the HOMO region (HOMO−1, HOMO−2). Contrastingly, both the HOMO and the LUMO were located on the cationic π-system in the case of the hexafluorophosphate compounds. The $PF_6^-$ anion possesses the low-lying orbitals as a result of the high electronegativity of fluorine and the strong P–F bonds. It refrains from contributing frontier orbitals in the vicinity of the HOMO region (Fig. S43–S46, SI). This difference is the root of the external heavy-atom effect as iodide's orbitals near the HOMO facilitate spin–orbit coupling with the cationic π-system's orbitals, which promotes intersystem crossing and phosphorescence emission.

Additionally, we compared the crystal structure and solid-state packing of **3-I** with that of **3-PF$_6$** (Fig. 4a and b). In **3-PF$_6$**, the distances between the two counter anions and the oxazole core were 2.924 Å and 2.867 Å. In **3-I**, these distances became 3.494 Å and 3.634 Å. The torsional angles between the phenyl rings and the oxazole core at C1, C2, C3, and C4 changed as well. The torsional angles for **3-PF$_6$** at C1, C2, C3, and C4 were 62.02°, 61.56°, 23.46°, and 74.24°, respectively. But when iodide was present as an anion, they were 67.98°, 72.88°, 13.49°, and 81.86°, respectively (Fig. 4a and b). Also, there was a significant alteration in the solid-state packing arrangement from hexafluorophosphate to iodide compounds. In the presence of the hexafluorophosphate anion, there was a twisted arrangement of the molecules, due to which the non-covalent interactions

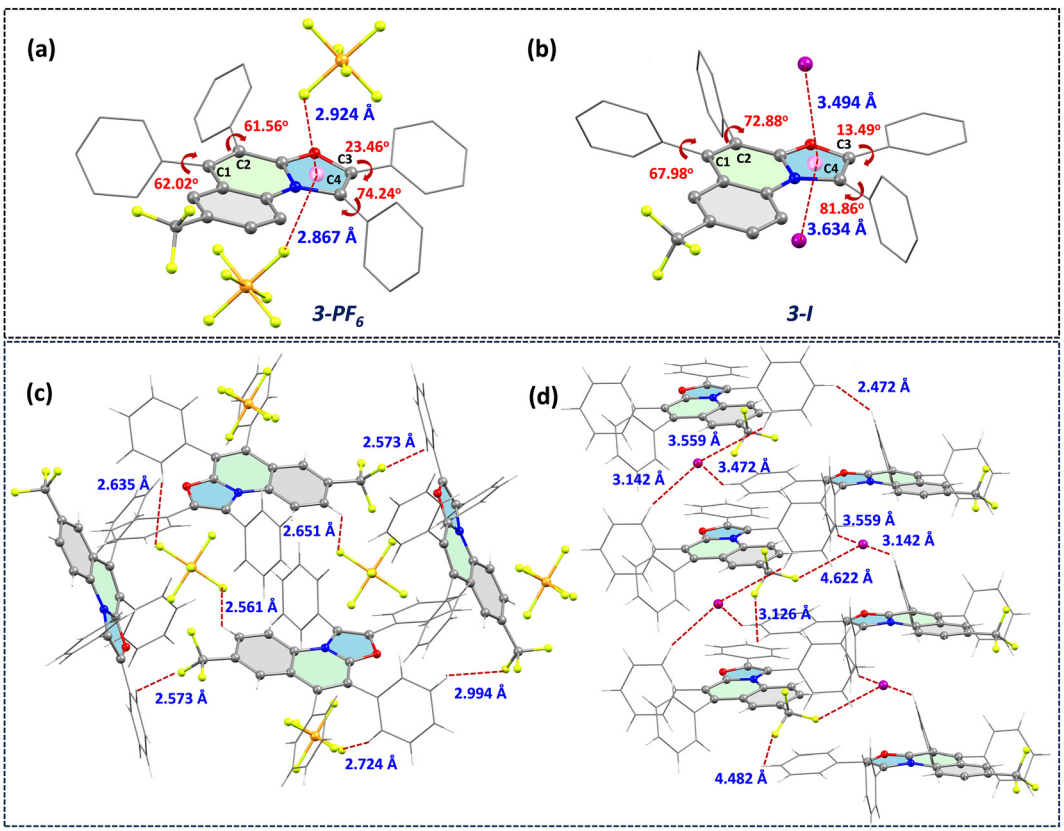


Fig. 4 (a) and (b) Crystal structure analysis and comparison of key parameters between **3-PF$_6$** and **3-I**. (c) Non-covalent interactions between the fluorine atoms of the hexafluorophosphate anion and the hydrogen atoms of the phenyl rings of **3-PF$_6$**. (d) Non-covalent interactions between the iodide anion and the hydrogen atoms of the phenyl rings of **3-I**.

between the hexafluorophosphate and hydrogen atoms of the phenyl rings were in the range of 2.5–2.7 Å (Fig. 4c). However, in the case of the iodide compound, such twisted molecular arrangement was absent. Only layered structures were identified, with non-covalent interactions between the iodide anion and hydrogen atoms of the phenyl groups in the range of 3.1–3.6 Å (Fig. 4d). The crystal structures of **1-I** and **2-I** were also analysed, where only one counter-anion was found to interact with the oxazole core (Fig. S34–S36, SI). Overall, the comparative analysis of the crystal structures and crystal-packing of both hexafluorophosphate and iodide salts provided crucial insights into the structure–property relationships, governing the changes in the photophysical properties. The crystallographic data revealed how different counter-anions influenced molecular packing and intermolecular distances, thereby providing a structural basis for the observed modifications of the spectroscopic features.

In summary, this work demonstrated the substantial impact of the counter-anion substitution on the photophysical properties of ring-fused annulated oxazolium salts in the solid state. The introduction of iodide as a counter-anion significantly altered the electronic structure of the cation–anion system. The higher-lying 5p orbitals of iodide dominated the frontier molecular orbitals, in contrast to hexafluorophosphate, whose deep-lying orbitals leave the cation to define the HOMO region. This orbital alignment facilitates strong spin–orbit coupling between iodide and the organic cation, thereby enabling efficient intersystem crossing. As a result, the anion–$\pi^+$ interaction-enabled external heavy atom effect of iodide played a crucial role in promoting the solid-state room-temperature phosphorescence in the iodide luminogens, in comparison to the solid-state fluorescence property of the hexafluorophosphate compounds. Furthermore, the feasibility of the reversible anion-exchange in the compounds opened up the possibility of achieving a solid-state fluorescence–phosphorescence switch. Future work is necessary to find the practical potential of these systems.

Financial support from ANRF (erstwhile SERB) (Grant No. CRG/2019/006038 and CRG/2022/005562) and IISER Bhopal is gratefully acknowledged. S. S. R. thanks UGC, S. J. thanks IISER Bhopal, and C. B. thanks CSIR for the doctoral fellowships.

## Conflicts of interest

There are no conflicts to declare.

## Data availability

The data supporting this article are included in the supplementary information (SI). Supplementary information: detailed experimental details; spectral data; computational data. See DOI: https://doi.org/10.1039/d5cc05870h.

CCDC 2495459, 2495460 and 2502118 contain the supplementary crystallographic data for this paper.[20a–c]

## References

1 M. Giese, M. Albrecht and K. Rissanen, *Chem. Rev.*, 2015, **115**, 8867.
2 B. L. Schottel, H. T. Chifotides and K. R. Dunbar, *Chem. Soc. Rev.*, 2008, **37**, 68.
3 A. J. Neel, M. J. Hilton, M. S. Sigman and F. D. Toste, *Nature*, 2017, **543**, 637.
4 J. Mei, N. L. C. Leung, R. T. K. Kwok, J. W. Y. Lam and B. Z. Tang, *Chem. Rev.*, 2015, **115**, 11718.
5 X. Sun, B. Zhang, X. Li, C. O. Trindle and G. Zhang, *J. Phys. Chem. A*, 2016, **120**, 5791.
6 J. Wang, X. Gu, H. Ma, Q. Peng, X. Huang, X. Zheng, S. H. P. Sung, G. Shan, J. W. Y. Lam, Z. Shuai and B. Z. Tang, *Nat. Commun.*, 2018, **9**, 2963.
7 E. Hakkarainen, H.-C. Lin, A. A. Nechaev, V. A. Peshkov, T. Eskelinen, K.-H. Chang, T.-H. Liao, P.-Y. Chen, I. O. Koshevoy, H.-W. Lin, P.-T. Chou and A. Belyaev, *Chem. Sci.*, 2025, **16**, 17261.
8 S. Garain, S. M. Wagalgave, A. A. Kongasseri, B. C. Garain, S. N. Ansari, G. Sardar, D. Kabra, S. K. Pati and S. J. George, *J. Am. Chem. Soc.*, 2022, **144**, 10854.
9 I. Partanen, O. Al-Saedy, T. Eskelinen, A. J. Karttunen, J. J. Saarinen, O. Mrózek, A. Steffen, A. Belyaev, P.-T. Chou and I. O. Koshevoy, *Angew. Chem., Int. Ed.*, 2023, **62**, e202305108.
10 D. Ghorai and J. Choudhury, *Chem. Commun.*, 2014, **50**, 15159.
11 C. Dutta, A. B. Sainaba and J. Choudhury, *Chem. Commun.*, 2019, **55**, 854.
12 C. Dutta, S. S. Rana and J. Choudhury, *ACS Catal.*, 2019, **9**, 10674.
13 P. Karak, S. S. Rana and J. Choudhury, *Chem. Commun.*, 2022, **58**, 133.
14 P. Karak and J. Choudhury, *Chem. Sci.*, 2022, **13**, 11163.
15 P. Karak, P. A. Sreelakshmi, B. Chakraborty, M. Pal, B. Khatua, A. L. Koner and J. Choudhury, *Angew. Chem., Int. Ed.*, 2023, **62**, e202310603.
16 S. S. Rana and J. Choudhury, *J. Am. Chem. Soc.*, 2024, **146**, 3603.
17 S. S. Rana and J. Choudhury, *Angew. Chem., Int. Ed.*, 2024, **63**, e202406514.
18 S. S. Rana, S. Manna and J. Choudhury, *Chem. Commun.*, 2024, **60**, 10942.
19 M. H. Chua, K. W. Shah, H. Zhou and J. Xu, *Molecules*, 2019, **24**, 2711.
20 (*a*) CCDC 2495459: Experimental Crystal Structure Determination, 2025, DOI: 10.5517/ccdc.csd.cc2prqpw; (*b*) CCDC 2495460: Experimental Crystal Structure Determination, 2025, DOI: 10.5517/ccdc.csd.cc2prqqx; (*c*) CCDC 2502118: Experimental Crystal Structure Determination, 2025, DOI: 10.5517/ccdc.csd.cc2pznhv.